



Neuroimaging Of Cold Allodynia Reveals A Central Disinhibition Mechanism Of Pain

This article was published in the following Dove Press journal:
Journal of Pain Research

Julia Forstenpointner ^{1,2,*}
 Andreas Binder ^{1,2,*}
 Rainer Maag ^{1,2}
 Oliver Granert ²
 Philipp Hüllemann ^{1,2}
 Martin Peller²
 Gunnar Wasner ^{1,2}
 Stefan Wolff³
 Olav Jansen³
 Hartwig Roman Siebner ^{2,4-6}
 Ralf Baron ^{1,2}

¹Division of Neurological Pain Research and Therapy, Department of Neurology, University Hospital Schleswig-Holstein, Kiel, Germany; ²Department of Neurology, University Hospital Schleswig-Holstein, Kiel, Germany; ³Institute of Radiology and Neuroradiology, University Hospital of Schleswig-Holstein, Kiel, Germany; ⁴Danish Research Centre for Magnetic Resonance, Centre for Functional and Diagnostic Imaging and Research, Copenhagen University Hospital Hvidovre, Hvidovre, Denmark; ⁵Department of Neurology, Copenhagen University Hospital Bispebjerg, Copenhagen, Denmark; ⁶Institute for Clinical Medicine, Faculty of Health and Clinical Sciences, University of Copenhagen, Copenhagen, Denmark

*These authors contributed equally to this work

Correspondence: Julia Forstenpointner
 Division of Neurological Pain Research and Therapy, Department of Neurology, University Hospital Schleswig-Holstein, Campus Kiel, Arnold-Heller-Str. 3, Haus 41, Kiel 24105, Germany
 Tel +49 431 500 23921
 Fax +49 431 500 23914
 Email julia.forstenpointner@uksh.de

Purpose: Allodynia refers to pain evoked by physiologically innocuous stimuli. It is a disabling symptom of neuropathic pain following a lesion within the peripheral or central nervous system. In fact, two different pathophysiological mechanisms of cold allodynia (ie, hypersensitivity to innocuous cold) have been proposed. The peripheral sensitization of nociceptive neurons can produce cold allodynia, which can be induced experimentally by a topical application of menthol. An alternative mechanism involves reduced inhibition of central pain processing by innocuous cold stimuli. A model to induce the latter type of allodynia is the conduction block of peripheral A-fiber input.

Patients and methods: In the presented study, functional MRI was used to analyze these two different experimental models of cold allodynia. In order to identify the underlying cerebral activation patterns of both mechanisms, the application of menthol and the induction of a mechanical A-fiber blockade were studied in healthy volunteers.

Results: The block-induced cold allodynia caused significantly stronger activation of the medial polymodal pain processing pathway, including left medial thalamus, anterior cingulate cortex, and medial prefrontal cortex. In contrast, menthol-induced cold allodynia caused significantly stronger activity of the left lateral thalamus as well as the primary and secondary somatosensory cortices, key structures of the lateral discriminative pathway of pain processing. Mean pain intensity did not differ between both forms of cold allodynia.

Conclusion: Experimental cold allodynia is mediated in different cerebral areas depending on the underlying pathophysiology. The activity pattern associated with block-induced allodynia confirms a fundamental integration between painful and non-painful temperature sensation, ie, the cold-induced inhibition of cold pain.

Keywords: A-fiber block, menthol, cold allodynia, fMRI

Introduction

How do central nociceptive structures become excessively sensitive to innocuous stimuli? Many patients with neuropathic pain, eg, postherpetic neuralgia or central pain, are hypersensitive to innocuous stimuli. For cold allodynia, two putative mechanisms have been postulated.¹ The first mechanism involves a sensitization of peripheral nociceptive structures. This peripheral sensitization mechanism can be modeled in humans by treating the skin with topical menthol. Cutaneous application of menthol leads to acute sensitization of peripheral cold-sensitive C-fibers, presumably by activation of the cold sensing transient receptor potential channel (TRPM8), which causes cold allodynia.²⁻⁵ Alternatively, cold allodynia can also be induced by a peripheral sensitization of A-delta fibers (ie, TRPA1) via natural toxins such as ciguatoxin or chemotherapeutics such as Oxaliplatin.^{6,7}

The second mechanism is based on the thermosensory disinhibition theory of pain generation. According to this concept, innocuous cold stimuli physiologically inhibit central processing of C-fiber nociceptive input. In humans, innocuous cold stimuli are transmitted centrally by cold-specific myelinated A δ -fibers, whereas noxious cold is conveyed via nociceptive cold-sensitive C-fibers. Inhibition of A-fiber input leads to “central disinhibition” of nociceptive pathways resulting in cold allodynia.^{8–10} This mechanism can be studied by inducing a mechanical conduction blockade of myelinated A-fibers in a cutaneous nerve.^{11–13} This model induces cold allodynia by impairing innocuous cold sensation and tactile perception but does not interfere with C-fiber function. Moreover, human microneurographic studies demonstrated that mechanical nerve compression produces a preferential A-fiber blockade without affecting the blood supply.^{13–15}

In humans, pain is processed via two main central pathways.¹⁰ The lateral pathway conveys innocuous thermoreceptive (cold-specific) as well as nociceptive activity.¹⁶ It projects to the primary and secondary somatosensory cortices as well as the dorsal part of the insula and is at least partially involved in the perception of sensory-discriminative dimensions of pain.^{16–18} In contrast, the medial pathway is preferentially activated by polymodal noxious stimuli (ie noxious cold, heat, and mechanical pressure) and involves the anterior cingulate cortex (ACC) implicating affective-motivational pain processing.^{19–21}

Therefore, in support of previously conducted studies, the following hypotheses were put forward (see Figure 1):

- (i) First, based on the two-pathway model of central pain processing, it was hypothesized that menthol-induced sensitization of peripheral nociceptors activates the thermoreceptive spinothalamic pathway as well as the polymodal nociceptive spinothalamic tract.
- (ii) Second, it was hypothesized that due to the inhibitory influence of the lateral pathway on neuronal processing in the medial polymodal nociceptive pathway, menthol should preferentially activate the lateral thalamus involved in discriminative coding of pain.
- (iii) Third, an A-fiber blockade that reduces innocuous cool sensation decreases neuronal activity in the lateral innocuous thermoreceptive spinothalamic pathway and results in central disinhibition of the medial spinothalamic polymodal nociceptive channel.

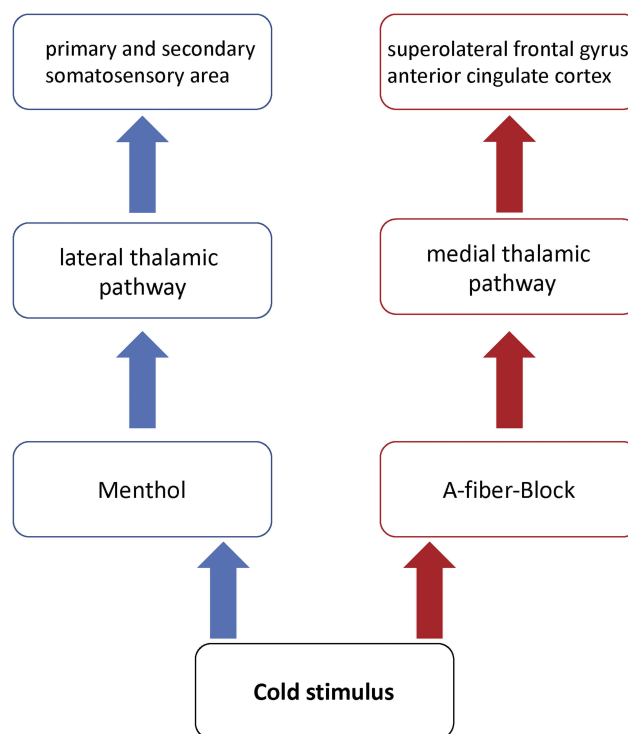


Figure 1 Hypothesized regions of activation.

Note: Displayed are the hypothesized regions of activation by cold stimuli, either in menthol pre-treated skin or in the area within the preferential A-fiber block.

Materials And Methods

Subjects

Eight healthy right-handed males (mean age: 26.6 years; age range: 23 to 35 years) participated in the study. Handedness was assessed by the German version of the Edinburgh Handedness Inventory.²² Participants were informed about the experimental procedures and were fully aware of the duration and intensity of cold pain that they would need to endure. Participants gave their written informed consent to the protocol. The study was approved by the local ethics committee of the University Hospital of Kiel and conducted according to the Declaration of Helsinki.

Experimental Design

Each participant underwent two experimental sessions which were performed on separate days at least a week apart in a randomized order. In both experiments, abnormal sensitivity to innocuous cold (ie, cold allodynia) was induced in the innervation territory of the right superficial radial nerve using two different techniques (menthol application, A-fiber blockade; see section “Procedures To Induce Cold Allodynia”). Thermal measurements and

stimulations were conducted at a defined $3 \times 3 \text{ cm}^2$ region at the back of the right hand between the proximal segments of the metacarpal bones I and II, ie, the innervation territory of the superficial radial nerve. In one session, menthol was topically applied to the skin, whereas in the other session, a mechanical blockade of the superficial radial nerve at the right forearm just proximal to the wrist was conducted. Apart from the technique used to induce cold allodynia, the experimental protocol was identical in both sessions.

The volunteers rested in the scanner room for at least 20 mins, and then thermal detection and pain thresholds were assessed. Thereafter, cold allodynia was induced by applying the individually determined cold pain threshold repetitively. Thereby the regional neuronal activity during the perception of innocuous and painful cold stimuli was measured using blood-oxygen level-dependent (BOLD) functional magnetic resonance imaging (fMRI). In addition, participants had to score the pain intensity and the quality of pain in between each cold stimulus (see sections “Psychophysiological Measurements” and “fMRI Study Design”).

After the fMRI measurements, the cold pain threshold was measured again to prove stability of the induced cold allodynia. To ensure comparability among measurements, all psychophysiological and fMRI measurements were performed in a supine position within the fMRI scanner. The room temperature was kept constant at 21°C .

Procedures To Induce Cold Allodynia

The menthol-induced allodynia was conducted according to the protocol of Wasner et al.² A 1 mL aliquot of a solution containing 400 mg of L-menthol (40%) dissolved in 90% ethanol (Hof-Apotheke, Kiel) was placed on a $3 \times 3 \text{ cm}^2$ gauze pad for 20 mins. The gauze pad was applied to the skin in the innervation territory of the right superficial radial nerve and covered by an adhesive film as well as fixed by a rubber band. After removing the pad, the skin was wiped with a swab to remove any remaining menthol.

Blockade of A-fibers was achieved by applying pressure to the right superficial radial nerve as described previously.¹¹ During the procedure, the hand rested in a semiprone position and a 2.5 cm wide rubber band was placed across the forearm just proximal to the wrist and loaded with a weight of 1.2 kg for a maximum period of 1.5 hrs.

Efficacy of A-fiber conduction blockade was assessed psychophysically within the innervation territory of the right superficial radial nerve, ie, on the radial part of the hand's dorsum, as described previously.² A shift in cold detection threshold below 10°C indicated a significant blockade of cold-specific A δ -fibers. An anesthesia for light mechanical touch was indicative for the inhibition of mechanosensitive A β -fiber afferents. In contrast, C-fiber function was unaffected; this was indicated by constant warm detection and heat pain thresholds. The A-fiber block is reversible within a few minutes upon lifting the weight from the nerve or a changed hand/forearm-position. Therefore, the positioning of the right arm was conducted accurately and the unaltered position during the experiment was visually monitored. Sufficiency of the conduction block during the study was also controlled by the measurement of the cold pain threshold at the end of each session.

Psychophysiological Measurements

Thermal perception thresholds (warm detection threshold (WDT), cold detection threshold (CDT), heat pain threshold (HPT), and cold pain threshold (CPT)) were measured by a thermal testing device (TSA II, Medoc, Ramat Yishai, Israel) prior to eliciting cold allodynia and to prove accuracy of the A-fiber blockade (see section “Procedures To Induce Cold Allodynia”). Additionally, cold pain thresholds were determined after menthol application, during A-fiber block and after fMRI sessions to validate cold allodynia stability throughout the experiment.^{2,3} A Peltier type thermode ($3 \times 3 \text{ cm}$) was applied exactly within the area of menthol application, which was within the territory of the right superficial radial nerve. The method of limits was used with a starting temperature of 32°C and a 1°C/s ramp velocity to apply either warm or cold stimuli. The volunteers were instructed to press a button immediately when the respective thermal sensation was perceived. Thresholds were determined as the average of three successive stimuli using an inter-stimuli interval of 3–5 s (randomized) for expected non-painful stimuli. An inter-stimulus interval of 20 s for expected painful stimuli was used to allow normalization of skin temperature at the test area after each thermal stimulus.

Intensity of cold-induced pain was quantified on a numeric rating scale during the fMRI scan (NRS 0–10; with 0 representing “no pain” and 10 being “the maximum imaginable pain”). The volunteers had to select a number indicative for their pain for each thermal stimulus with the

left hand (Figure 2, R marks) (see section “MRI acquisition and fMRI data analysis”).²

Thereafter, an identical thermal stimulus as used during the fMRI scan was applied and participants had to determine the subjective quality of cold allodynia using the McGill Pain Questionnaire (MPQ).^{24,25}

fMRI Study Design

An fMRI block design which consisted of alternating periods (12 s) of neutral and cold thermal stimulations was used. The Peltier type thermode (3 × 3 cm) was placed at the area of experimentally induced cold allodynia, ie, within the area of menthol application or within the territory of the right superficial radial nerve. The thermode was placed on the skin throughout all fMRI sessions in order to minimize perceptual effects of air movement. During neutral thermal stimulation, the thermode applied a constant temperature of 32°C. The cold thermal stimulation was adjusted to the individual cold pain threshold. In total, 20 cold stimuli were applied per fMRI run. It included 4 different types of cold stimuli, which were set at 3°C or 6°C above or below the individual cold pain threshold (+6°C, +3°C, -3°C, and -6°C) after induction of cold allodynia. Each cold stimulus was applied five times in a pseudorandom order and counterbalanced in terms of relative differences of consecutive cold stimuli. Immediately after a cold stimulus, volunteers had to rate the pain intensity of the stimulus on the NRS scale. The rating

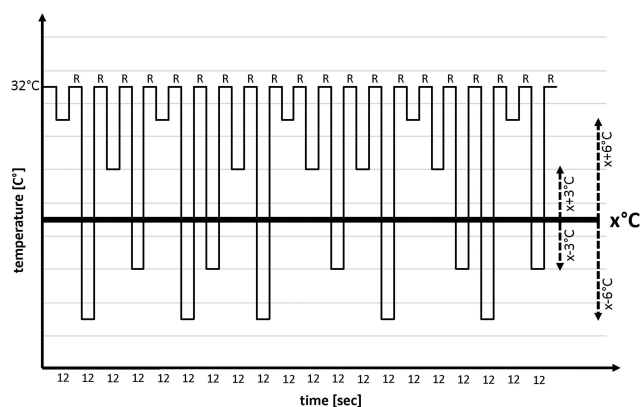


Figure 2 fMRI stimulation paradigm.

Notes: A blocked fMRI design consisting of 12s epochs of alternating neutral and cold stimuli was applied. Each fMRI session comprised four different degree modalities, which were set at 3°C or 6°C above (X+6°C, X+3°C; ie, innocuous) or below (X-3°C and X-6°C; ie, nocuous) the individual cold pain threshold (X) after induction of cold allodynia. Each cold stimulus was applied five times (ie, in total 20 cold stimuli) in a pseudorandom order and counterbalanced in terms of relative differences of consecutive cold stimuli. Immediately after a cold stimulus and reaching the thermode's baseline temperature of 32°C, volunteers had to rate (ie, R marks) the pain intensity of the stimulus on the NRS with their left hand.

was recorded by an investigator present in the MR scanner room.

MRI Acquisition And fMRI Data Analysis

MRI was conducted with a 1.5 T MR scanner (Gyroscan, Philips Intera 1.5 T, Germany). To exclude structural abnormalities, T1-weighted 3-D gradient-echo images of the whole brain were acquired (TR = 7.4 ms, TE = 3.6 ms, 60 slices, matrix: 208 × 129 mm). BOLD fMRI was performed using a gradient-echo, echo-planar-imaging (EPI) sequence with TE = 50 ms, TR = 3000 ms, flip angle = 90°, FOV = 230 mm, and a 64×64 matrix. Each brain volume covered the entire brain (33 axial slices with a slice thickness of 3 mm and a gap of 0.5 mm). The fMRI measurements were divided into two consecutive fMRI runs (771s per run). In total, 257 brain volumes were acquired per fMRI run.

fMRI data were analyzed using SPM12 software (www.fil.ion.ucl.ac.uk/spm). The first three scans of each fMRI run were excluded from data analysis because of the non-equilibrium state of magnetization. The effect of head motion across time was corrected by realigning all scans to the mean of the images after the first realignment. Realigned images were spatially normalized to a standard EPI template. Normalized images were spatially smoothed with a Gaussian kernel of 8 mm full-width at half-maximum to reduce intersubject differences in anatomy and enable the application of the Gaussian random field theory.

A first-level analysis was performed individually for each subject and experimental session based on the general linear model.²⁶ Task-related changes in BOLD signal were estimated at each voxel by modeling the onsets and duration of the cold stimuli as delta functions convolved with a hemodynamic response function (HRF). Each of the four stimuli (+6°C, +3°C, -3°C, and -6°C with respect to the individual cold pain threshold) and motor responses with the left hand (pain rating) were modeled as separate regressors. Regression coefficients (parameter estimates) for all regressors were estimated in a subject-specific fixed-effects model.²⁶ Low-frequency drifts in BOLD signal were removed by a high pass filter with a cut-off of 128s. Using appropriate linear contrasts, contrast images of interest were selected for each participant, including BOLD signal changes associated with each type of cold stimuli.

Group analysis (second level) employed a random-effects analysis treating subjects as a random variable. The individual contrast images were entered into a two-factorial ANOVA with the factors baseline vs stimulation condition

(2 levels, prior menthol/fiber block-induced allodynia vs during menthol/fiber block-induced allodynia). The two types of stimuli above and below the cold pain threshold were combined in a weighted model to achieve sufficient statistical power for analysis. Contrasts of the two types of allodynia to baseline and contrasts of both types of allodynia were calculated. Due to possible conflicting motor responses induced by the pain rating during the baseline condition (see section “fMRI Study Design”), the first 4 s were discarded from the analysis. Statistical threshold was set at an uncorrected p-value of <0.001 . Additionally, a small volume correction was applied in target regions (ie, hypothesized areas of activation). Clusters showing significant changes in BOLD signal were characterized in terms of cluster size (number of voxels per cluster at an extent threshold of $p < 0.001$) and the voxel showing peak difference (*t*-value and stereotactic coordinates).

Statistical Analyses Of Psychophysical Data

The Wilcoxon test and the Mann–Whitney U-Test were used to compare psychophysical data, thermal thresholds, and pain intensity. Psychophysical data are presented as mean $[\pm$ standard deviation]. P values of <0.05 were regarded as statistically significant.

Results

Cold Allodynia

Topical menthol application and nerve conduction block induced a significant increase of sensitivity towards cold pain as compared to baseline thresholds (menthol: $\Delta=13.4^{\circ}\text{C}$ $[\pm 3.8]$, $p = 0.006$; fiber block: $\Delta=10.6^{\circ}\text{C}$ $[\pm 4.4]$, $p = 0.006$; Figure 3). In all volunteers, mechanical

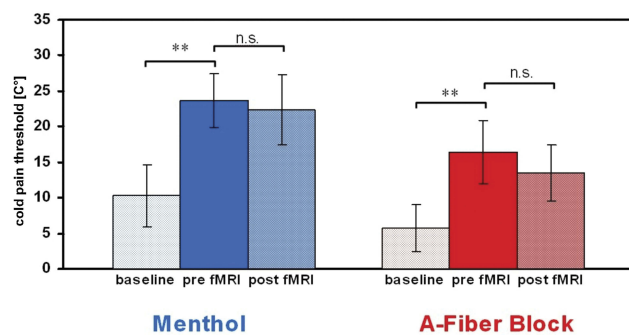


Figure 3 Mean cold pain thresholds (CPT) of experimental-induced cold allodynia. **Note:** Both interventions induced a significant decrease in CPT that persisted throughout the fMRI measurements (** $p < 0.01$). **Abbreviation:** n.s., not significant.

compression of the superficial radial nerve induced an effective blockade of cold-specific A δ -fibers (CDT 30.8°C $[\pm 0.9]$ vs 6.0°C $[\pm 3.2]$, $p = 0.006$) and A β -fibers according to the criteria set while the C-fiber-mediated warm detection and heat pain threshold did not change significantly (WDT 33.4°C $[\pm 0.2]$ vs 33.9°C $[\pm 0.9]$, $p = 0.6$; HPT 44.9°C $[\pm 2.1]$ vs 44.3°C $[\pm 1.4]$, $p = 0.5$). Psychophysiological measurements showed no significant change of the cold pain threshold before and after fMRI of each condition ($p > 0.1$; Figure 3) indicating stable cold allodynia throughout the experiment. Warm and cold detection as well as heat pain thresholds at baseline did not differ significantly between the two interventions (CDT 31.0°C $[\pm 0.2]$ vs 30.8°C $[\pm 0.9]$; WDT 33.5°C $[\pm 0.6]$ vs 33.4°C $[\pm 0.7]$; HPT 43.1°C $[\pm 3.16]$ vs 44.9°C $[\pm 2.1]$ ($p > 0.1$)), whereas the sensitivity towards cold pain was lower in the A-fiber block session at baseline (CPT 10.3°C $[\pm 4.4]$ vs 5.8°C $[\pm 3.3]$; $p = 0.02$).

Neuroimaging

Contrasting neuronal activity evoked by both types of cold allodynia indicated that block-induced allodynia was associated with prominent significant increases in the BOLD signal in the left medial thalamus, anterior cingulate cortex in the bilateral medial and superior frontal cortex (Figure 4; Table 1). In contrast, cold allodynia following topical menthol application produced significantly stronger activation of the left lateral thalamus as well as primary and secondary somatosensory cortices (Figure 4, Table 2). The results of contrast analysis of baseline versus stimulation for each type of cold allodynia are displayed in Tables 1 and 2.

Pain Intensity And Quality

The cold pain intensity ratings between menthol application and nerve conduction block did not show significant differences (menthol: 2.8 $[\pm 0.7]$, A-fiber block: 2.3 $[\pm 0.6]$, $p \geq 0.1$ (NRS 0–10)), Figure 5. The stimulus response indicated a graded NRS rating with respect to thermal stimuli (ie, +6, +3, –3, and –6). Further on, a correlation analysis demonstrated a significant correlation of the NRS ratings and the thermal stimuli in both conditions (Spearman-Rho: A-fiber block [$\text{Rho}=0.880$, $p < 0.000$]; Menthol [$\text{Rho}=0.840$, $p < 0.000$]). No subject reported spontaneous pain during the fMRI sessions.

As expected A-fiber block-induced cold allodynia was rated more often as “burning” and/or “hot” (8/8 subjects) whereas only 3 of 8 subjects reported such sensation during menthol-induced cold allodynia. In contrast, menthol-

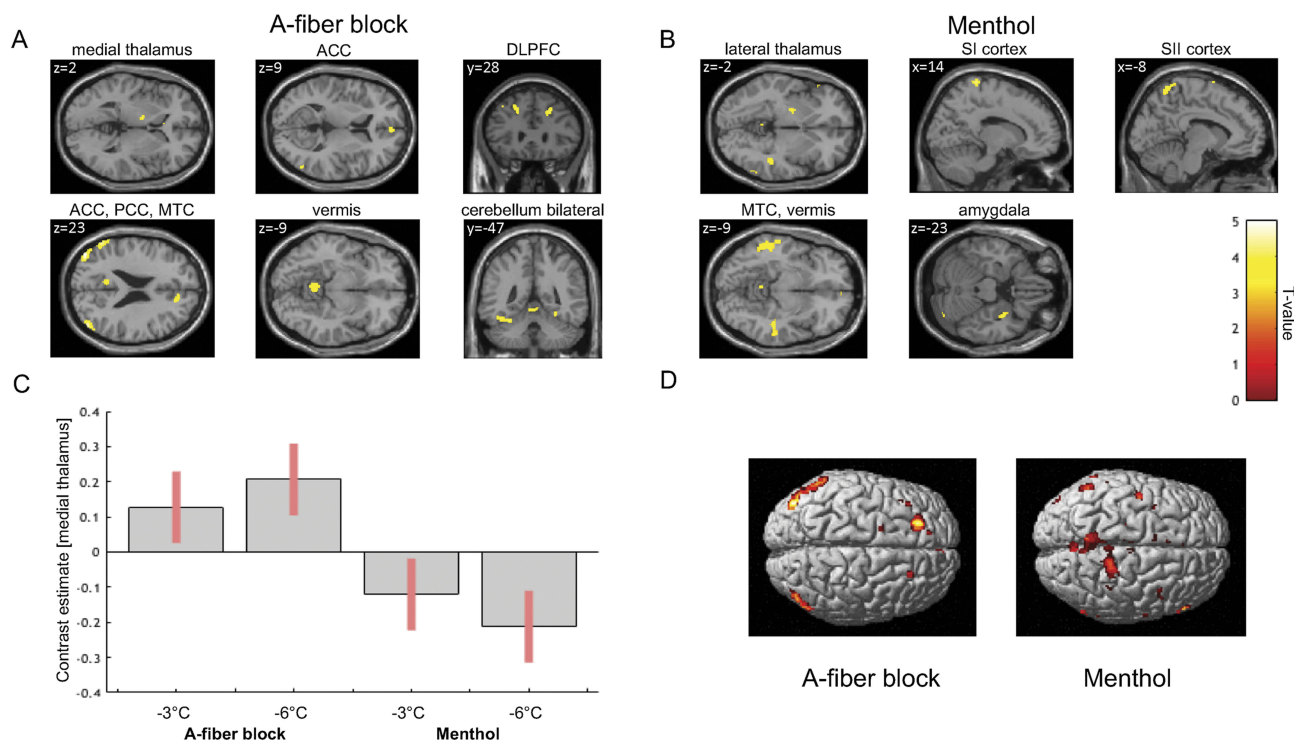


Figure 4 Differences in regional neuronal activity during cold allodynia induced by topical menthol application or A-fiber block.

Notes: (A) The A-fiber block-induced cold allodynia indicates a preferential activation of the medial thalamus and prefrontal cortical areas. (B) The menthol-induced cold allodynia causes a stronger activation of the lateral thalamus as well as SI and SII cortical regions. (C) The bar graph indicates the mean change in BOLD signal ($\pm 95\%$ confidence interval) of the medial thalamic region. The activation change during cold stimuli at -3°C and -6°C was compared between both types of cold allodynia models. (D) SPMs of cortical surface areas indicate a stronger activation of prefrontal areas during block-induced allodynia relative to the pronounced activation of SI and SII regions in menthol-induced allodynia. SPMs are thresholded at $p < 0.001$.

induced allodynia was described as “cold” and/or “freezing” in 8/8 subjects, whereas none did during A-fiber block. The McGill pain questionnaire showed no significant differences in the affective ($0.04 [\pm 1.14]$ vs $0.04 [\pm 1.14]$; $p = 1$) but in the sensory ($7.15 [\pm 3.86]$ vs $11.41 [\pm 6.38]$; $p = 0.045$) subscores and a non-significant trend in the evaluative ($9.88 [\pm 8.15]$ vs $5.51 [\pm 5.05]$; $p = 0.09$) subscore. The latter includes the terms “cold” and “freezing” (menthol-induced cold allodynia) and the sensory subscore the ratings for “hot” and “burning” (A-fiber block-induced cold allodynia). The pain rating index (PRI) showed no significant difference (menthol: $6.57 [\pm 0.92]$ vs block: $6.75 [\pm 0.92]$; $p = 0.46$).

Discussion

The presented study demonstrates that cold allodynia induces a preferential activation of characteristic brain regions depending on the underlying mechanism. Cold allodynia activates a set of brain regions that have previously been implicated in the processing of noxious cold stimuli, including the anterior cingulate cortex and thalamus.^{27–29} Interestingly, block-induced allodynia

revealed greater activation in three important areas of pain processing, the medial thalamus, the ACC, and the prefrontal cortex. Vice versa, menthol-induced allodynia led to a stronger activation of the lateral thalamus as well as primary and secondary somatosensory cortices. Critically, the differences in neuronal activity in the two models presented cannot be attributed to differences in pain intensity due to comparable mean pain intensity ratings for both types of cold allodynia. These findings imply that cold allodynia has two preferential neuronal representations in the human brain.

The differences in activation patterns shed new light on the mechanisms of cold allodynia. As outlined in the introduction, menthol-induced allodynia is attributed to peripheral sensitization resulting in an increased nociceptive C-fiber input. In contrast, mechanical nerve block does not affect C-fiber input but blocks A-fiber input from the periphery. Though the brain receives less sensory input during A-fiber block, ACC and frontal cortex showed increased activity levels during thermal stimulation. These findings provide direct evidence for the thermosensory disinhibition theory of pain generation.^{8,10,11,16}

Table 1 Regions Of Cerebral Activations During A-Fiber Blockade

	AAL Label				t-Value	Cluster Size [Voxels]	Brodmann Area [BA]				
	Side	X (mm)	Y (mm)	Z (mm)							
Thalamus ^a	Left	-12.0	-4.0	+2.0	3.76	10	-				
Caudate nucleus	Left	-14.0	-2.0	+20.0	4.50	38	-				
Medial frontal gyrus (DLPFC)	Left	-40.0	+26.0	+46.0	3.80	13	BA 09				
Medial frontal gyrus (DLPFC) ^a	Right	+22.0	+26.0	+38.0	5.08	67	BA 09				
Superolateral frontal gyrus (DLPFC) ^a	Left	-20.0	+34.0	+42.0	5.29	219	BA 09				
Superolateral frontal gyrus (DLPFC) ^b	Left	-12.0	+46.0	+52.0	3.68	10	BA 09				
Superolateral frontal gyrus (DLPFC) ^b	Left	-14.0	+44.0	+54.0	3.62	10	BA 09				
Superolateral frontal gyrus (DLPFC)	Right	+6.0	+56.0	+12.0	4.38	38	BA 10				
ACC ^a	Right	+14.0	+40.0	+22.0	4.60	45	BA 32				
PCC	Left	-6.0	-68.0	+20.0	4.15	141	BA 31				
PCC ^b	Left	-8.0	-52.0	+24.0	4.05	141	BA 23				
PCC	Right	+10.0	-52.0	+34.0	3.94	26	-				
PCC ^b	Right	+12.0	-54.0	+14.0	3.80	24	BA 30				
Middle temporal gyrus	Left	-54.0	-58.0	+23.0	1.94	365	BA 21				
Middle temporal gyrus	Right	+56.0	-68.0	+18.0	4.19	221	BA 39				
Middle temporal gyrus ^b	Right	+52.0	-60.0	+16.0	4.09	221	BA 37				
Angular gyrus	Left	-52.0	-68.0	+32.0	3.84	365	BA 39				
Middle occipital gyrus	Left	-42.0	-80.0	+26.0	5.26	365	BA 39				
Middle occipital gyrus	Right	+48.0	-78.0	+22.0	4.88	221	BA 39				
Vermis		-2.0	-52.0	-10.0	4.14	84					
Cerebellum	Left	-16.0	-50.0	-16.0	3.67	12	BA 19				
Cerebellum	Left	-32.0	-48.0	-22.0	4.40	113	BA 37				
Fusiform	Left	-42.0	-42.0	-20.0	5.19	113	BA 37				
Fusiform	Right	+28.0	-44.0	-14.0	3.60	24	BA 37				
Fusiform ^b	Right	+26.0	-42.0	-16.0	3.49	24	BA 37				
Fusiform ^b	Right	+42.0	-16.0	-20.0	4.11	12	BA 20				
Small volume correction											
					Cluster			Peak			
	X	Y	Z	p-set	p(FWE-corr)	equivk	p(unc)	p(FWE-corr)	T	equivZ	p(unc)
Thalamus left (radius of VOI 8 mm)	-12	-4	2	0.032	0.016	10	0.500	0.010	3.76	3.51	0.000
DLPFC left (radius of VOI 8 mm)	-20	34	42	0.032	0.000	171	0.010	0.000	5.29	4.69	0.000
DLPFC right (radius of VOI 8 mm)	22	26	38	0.032	0.003	66	0.087	0.000	5.08	4.53	0.000
ACC (radius of VOI 8 mm)	14	40	22	0.032	0.005	45	0.151	0.001	4.6	4.18	0.000

Notes: ^aThresholds (unc. $p < 0.001$) and small volume corrections of target regions. ^bClusters with a size of >10 voxels and a maximum of 2 sub-peaks for each region.
Abbreviations: ACC, anterior cingulate cortex; PCC, posterior cingulate cortex; DLPFC, dorsolateral prefrontal cortex.

In primates, thermosensory lamina I dorsal horn neurons project via the lateral spinothalamic tract to two main sites:^{8,10,30} a lateral thalamic relay nucleus (VMpo) that

projects to the dorsal posterior insular cortex, and higher cortical centers (lateral system) and a medial thalamic area (MDvc) that projects to the anterior cingulate cortex and

Table 2 Regions Of Cerebral Activations During Menthol Application

	AAL Label				t-Value	Cluster Size [Voxels]	Brodmann Area [BA]
	Side	X (mm)	Y (mm)	Z (mm)			
Thalamus ^a	Left	-22.0	-6.0	-2.0	4.15	34	-
Thalamus	Right	+18.0	-20.0	+2.0	3.58	13	-
Amygdala	Right	+34.0	+0.0	-22.0	4.08	60	-
Hippocampus	Left	-26.0	-24.0	-10.0	3.50	15	-
Hippocampus	Right	+26.0	-8.0	-18.0	3.79	12	-
Medial frontal gyrus (DLPFC)	Right	+48.0	+10.0	+52.0	3.46	15	BA 06
Medial frontal gyrus (DLPFC) ^b	Right	+42.0	+8.0	+52.0	3.43	15	BA 06
Inferior frontal gyrus	Right	+60.0	+30.0	+10.0	4.69	52	BA 45
Inferior frontal gyrus ^b	Right	+58.0	+32.0	+16.0	4.55	52	BA 45
Inferior frontal gyrus ^b	Right	+56.0	+34.0	+18.0	4.11	52	BA 45
Precentral gyrus	Left	-36.0	+4.0	+40.0	3.88	20	BA 06
PCC	Right	+4.0	-44.0	+26.0	3.69	19	BA 26
SI ^a	Left	-46.0	-10.0	+36.0	4.29	64	BA 03
SI	Right	+20.0	-36.0	+80.0	5.42	318	BA 03
SI ^b	Right	+28.0	-32.0	+76.0	4.46	318	BA 03
Paracentral lobule	Right	+2.0	-40.0	+74.0	3.79	318	BA 04
SII ^a	Left	-6.0	-56.0	+68.0	4.62	318	BA 07
SII ^b	Left	-6.0	-58.0	+64.0	4.53	318	BA 07
SII ^b	Left	-10.0	-54.0	+72.0	4.39	318	BA 05
SII	Right	+4.0	-60.0	+68.0	4.83	318	BA 05
SII ^b	Right	+2.0	-58.0	+66.0	4.67	318	BA 07
SII ^b	Right	+2.0	-70.0	+56.0	4.53	46	BA 07
Middle temporal gyrus	Left	-54.0	-16.0	-16.0	4.73	312	BA 20
Middle temporal gyrus ^b	Left	-54.0	-44.0	-10.0	4.50	312	BA 20
Middle temporal gyrus ^b	Left	-54.0	-34.0	-8.0	4.26	312	BA 21
Middle temporal gyrus	Right	+56.0	-28.0	-8.0	3.58	135	BA 20
Middle temporal gyrus ^b	Right	+50.0	-40.0	+6.0	3.44	135	BA 21
Middle temporal gyrus ^b	Right	+62.0	-58.0	+4.0	3.95	31	BA 37
Superior temporal gyrus	Left	-58.0	-46.0	+14.0	3.43	33	BA 22
Superior temporal gyrus ^b	Left	-56.0	-40.0	+24.0	3.63	13	BA 48
Supra marginal gyrus	Left	-50.0	-46.0	+32.0	3.53	65	BA 48
Angular gyrus	Left	-56.0	-56.0	+36.0	4.61	65	BA 39
Vermis		-2.0	-46.0	-6.0	3.92	26	BA 27

Small volume correction

	Cluster				Peak						
	X	Y	Z	p-set	p(FWE-corr)	equivk	p(unc)	p(FWE-corr)	T	equivZ	p(unc)
Thalamus left (radius of VOI 8 mm)	-22	-6	-2	0.032	0.007	32	0.218	0.002	4.15	3.93	0.000
SII left (radius of VOI 8 mm)	-6	-56	68	0.032	0.003	69	0.079	0.001	4.62	4.33	0.000
	-6	-58	64	0.032				0.001	4.53	4.25	0.000
	-10	-54	72	0.032				0.001	4.39	4.13	0.000
	0	-54	66	0.032				0.004	4.03	3.82	0.000
SI left (radius of VOI 8 mm)	-46	-10	36	0.032	0.003	61	0.096	0.002	4.29	4.05	0.000

Notes: ^aThresholds (unc. p<0.001) and small volume corrections of target regions during menthol application. ^bClusters with a size of >10 voxels and a maximum of 2 sub-peaks for each region.

Abbreviations: PCC, posterior cingulate cortex; SI, primary somatosensory cortex; SII, secondary somatosensory cortex; DLPFC, dorsolateral prefrontal cortex.

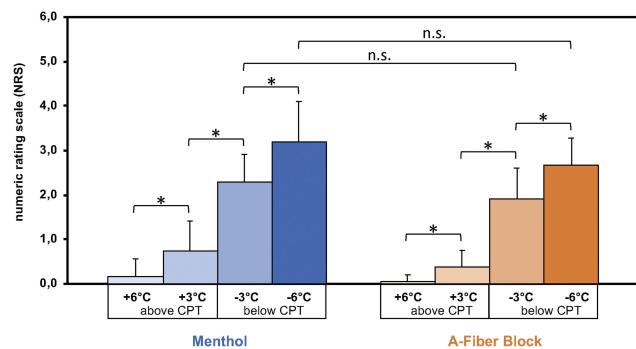


Figure 5 Mean pain intensity during experimental-induced cold allodynia.

Notes: Menthol-induced allodynia was associated with slightly higher pain intensities as compared to the A-fiber block condition. Further on, the results indicate a graded NRS response with respect to the different test stimuli (ie, +6, +3, -3, and -6). Mean pain intensity scores of the cold allodynia stimuli (ie, -3 and -6) were 2.8 [\pm 0.7] after topical application of menthol versus 2.3 [\pm 0.6] during A-fiber block on a numeric rating scale ranging from 0 (no pain) to 10 (maximal pain). * p <0.05. **Abbreviation:** n.s., not significant.

prefrontal areas (medial system). The lateral pathway conveys both, innocuous thermoreceptive (cold-specific) and nociceptive activity.^{8,16} The medial pathway is preferentially activated by polymodal noxious stimuli, ie, noxious cold, heat, and mechanical pressure. The cold stimulation in the menthol model activates the thermoreceptive spinothalamic neurons as well as polymodal nociceptive spinothalamic neurons, demonstrated by relative stronger activation of the lateral thalamus. Blocking the lateral innocuous thermoreceptive cooling channel selectively (A-fiber block, impairment of cold sensation) resulted in a profound increase in cold-induced activity within the medial system. This indicates that activity in the innocuous thermoreceptive system normally inhibits activity in the medial polymodal nociceptive pathway. Clinically, a disbalance of this regulatory system caused, eg, by a lesion within lateral system, is thought to lead to central pain.⁸ Interestingly, one study also indicated that an infarction of the Vc (ventral caudal thalamic nucleus), a portion of the lateral thalamic pathway, leads to central poststroke pain.³¹

Neuroimaging studies have contributed increasing knowledge to facilitate the understanding on pain processing.³²⁻³⁴ Thereby, thermal allodynia has been investigated in experimental pain models^{32,35} and in neuropathic pain patients.³⁶⁻⁴⁰ In an early positron emission tomography (PET) study, Craig and collaborators presented the thermal grill illusion (TGI) paradigm (ie, the application of non-painful cold stimuli with spatially interlaced non-painful warm stimuli). It was shown that the TGI sensation in healthy volunteers resembled the burning sensation of cold pain. Moreover, it was postulated to rely

on the mechanism of central disinhibition by a predominant activation of the anterior cingulate cortex.¹⁰ These results supported the hypothesis of physiological central inhibition of pain processing by innocuous cold sensation and were further confirmed by findings in detailed studies investigating the TGI paradigm.⁴¹ The present study extends these findings by showing that increased neuronal activity in the prefrontal cortex and medial thalamus are neuronal substrates for the central inhibition of pain. Moreover, our results are in line with a functional neuroimaging study of cold allodynia in patients with spinal lesions due to syringomyelia, in trigeminal neuropathy, CRPS patients and mixed neuropathic pain syndromes showing a stronger activation of the ACC and/or prefrontal areas.³⁶⁻⁴⁰ However, one study compared physiological cold pain and menthol-induced cold allodynia and indicated additional bilateral recruitment of prefrontal cortices,⁴² that seems to be further activated during block-induced allodynia as shown in our study. Thus, the present results indicate a fundamental integration between pain and temperature sensation, ie, the cold-induced inhibition of pain. A-fiber block disinhibits activity in the ascending polymodal nociceptive channel. The locus of unmasked activity is in the medial thalamus, the anterior cingulate, and prefrontal areas.

In the two models, innocuous cold stimuli produced cold allodynia of equal intensity, but the pain quality was different. In the nerve block model, participants rated the evoked sensation as hot and burning. In contrast, allodynia induced in the menthol-sensitized skin was described as freezing and cold, in both conditions without a considerable affective component. These ratings replicate previous work^{9,14} describing the quality of cold pain as burning and is well known from patients with post-stroke central pain syndromes reporting a burning pain sensation often within an area of impaired discriminative thermal sensation.^{39,43,44}

Finally, the question remains why the induction of experimental cold allodynia either by an A-fiber blockade or menthol application has been predominantly observed in healthy volunteers and not in patients. Several studies indicated that in patients these pathways seem to be attenuated. For example, the topical treatment with TRPM8 or TRPA1 agonists do not provoke pain in patients with neuropathic cold allodynia.^{45,46} Topical menthol has even been shown to reduce pain in carpal tunnel syndrome in a placebo-controlled trial.⁴⁷ In fact, there is no mentioning of TRP-independent mechanisms of cold transduction, including cold-sensitive potassium channels and resurgent

currents in sodium channels.^{48–51} Additionally, another study assessing oxaliplatin-induced cold hyperalgesia demonstrated a complete diminishing of cold allodynia via a preferential A-fiber blockade.⁷ In light of this evidence, these results need to be interpreted carefully with regard to clinical implications. In fact, a constant (ie, chronic) depolarization of structures conveying cold allodynia presumably leads to an altered processing of cold stimuli as compared to an acute induction of cold allodynia.⁵² Therefore, our observations suggest that future investigations should aim to scrutinize the difference of cerebral activation patterns in cold allodynia surrogate models between patients and healthy volunteers. This may reveal further differences in the complex processing of cold pain sensations and may contribute to the development of new therapeutic strategies.

Disclosure

RB, GW, AB and RM were supported by the German Federal Ministry of Education and Research (BMBF), German Research Foundation DFNS (grant 01 EM 0504) and an unrestricted educational grant from Pfizer, Germany. HS was supported by the BMBF (grant 01 GO 0511). AB reports grants and personal fees from Pfizer, personal fees from Grünenthal, Allergan and Mundipharma, during the conduct of the study; honoraria from Astellas, Allergan, Bayer, Boehringer-Ingelheim, Grünenthal, and Pfizer; and he participated in advisory boards of Astellas, Boehringer-Ingelheim, Genzyme, and Grünenthal. RM reports grants and personal fees from Pfizer and personal fees from Grünenthal and Genzyme, during the conduct of the study. JF reports personal fees and non-financial support from Grünenthal GmbH and Sanofi Genzyme, personal fees from Bayer, non-financial support from Novartis, outside the submitted work. PH reports speaking fees from Pfizer and Genzyme; travel reimbursement from Grünenthal; and grants from BMBF and Medoc, outside the submitted work. MP, OG, GW, SW and OJ reports no conflicts of interest in this work. HRS has received honoraria from Novartis, Sanofi-Genzyme, Elsevier Publishers and Springer Publishing; reports grants from Lundbeckfonden, during the conduct of the study. HRS professorship is sponsored by Lundbeckfonden. RB reports personal fees from Pfizer, Genzyme GmbH, Grünenthal GmbH, Mundipharma, Sanofi Pasteur, Medtronic Inc. Neuro-modulation, Eisai Co.Ltd., Lilly GmbH, Boehringer Ingelheim Pharma GmbH&Co.KG, Astellas, Desitin, Teva Pharma, Bayer-Schering, MSD GmbH, Seqirus, Novartis, TAD Pharma GmbH, Allergan, Sanofi Pasteur, Medtronic, Bristol-Myers Squibb, Biogenidec,

AstraZeneca, Merck, Abbvie, Daiichi Sankyo, Glenmark Pharmaceuticals, Genentech, Galapagos NV, Kyowa Kirin GmbH, Vertex Pharmaceuticals Inc., Biotest AG, Celgene, Theranexus, Bayer AG, Akcea, and Asahi Kasei Pharma; grants from Pfizer, Genzyme GmbH, Grünenthal GmbH, Mundipharma, German Research Network on Neuropathic Pain (01EM0903), NoPain system biology (0316177C), German Research Foundation (DFG), EU-Project IMI Paincare, Novartis, German Federal Ministry of Education and Research (BMBF): member of the ERA_NET NEURON/IM-PAIN Project (01EW1503). Member of the EU Project No 633491: DOLORisk. Member of the IMI “Europain” collaboration and industry members of this are: Astra Zeneca, Pfizer, Esteve, UCB-Pharma, Sanofi Aventis, Grünenthal GmbH, Eli Lilly and Boehringer Ingelheim Pharma GmbH&Co.KG.

References

1. Baron R, Binder A, Wasner G. Neuropathic pain: diagnosis, pathophysiological mechanisms, and treatment. *Lancet Neurol.* 2010;9(8):807–819. doi:10.1016/S1474-4422(10)70143-5
2. Wasner G, Schattschneider J, Binder A, Baron R. Topical menthol—a human model for cold pain by activation and sensitization of C nociceptors. *Brain.* 2004;127(Pt 5):1159–1171. doi:10.1093/brain/awh134
3. Namer B, Seifert F, Handwerker HO, Maihofner C. TRPA1 and TRPM8 activation in humans: effects of cinnamaldehyde and menthol. *Neuroreport.* 2005;16(9):955–959. doi:10.1097/00001756-200506210-00015
4. Su L, Shu R, Song C, et al. Downregulations of TRPM8 expression and membrane trafficking in dorsal root ganglion mediate the attenuation of cold hyperalgesia in CCI rats induced by GFRalpha3 knock-down. *Brain Res Bull.* 2017;135:8–24. doi:10.1016/j.brainresbull.2017.08.002
5. Hatem S, Attal N, Willer JC, Bouhassira D. Psychophysical study of the effects of topical application of menthol in healthy volunteers. *Pain.* 2006;122(1–2):190–196. doi:10.1016/j.pain.2006.01.026
6. Eisenblatter A, Lewis R, Dorfler A, Forster C, Zimmermann K. Brain mechanisms of abnormal temperature perception in cold allodynia induced by ciguatoxin. *Ann Neurol.* 2017;81(1):104–116. doi:10.1002/ana.24841
7. Forstenpointner J, Oberlojer VC, Naleschinski D, et al. A-fibers mediate cold hyperalgesia in patients with oxaliplatin-induced neuropathy. *Pain Pract.* 2018;18(6):758–767. doi:10.1111/papr.12670
8. Craig AD. Mechanisms of thalamic pain. In: Henry JL, Panju A, Yashpal K, editors. *Central Neuropathic Pain: Focus on Poststroke Pain.* Seattle: IASP Press; 2007:81–100.
9. Craig AD, Bushnell MC, Zhang ET, Blomqvist A. A thalamic nucleus specific for pain and temperature sensation [see comments]. *Nature.* 1994;372(6508):770–773. doi:10.1038/372770a0
10. Craig AD, Reiman EM, Evans A, Bushnell MC. Functional imaging of an illusion of pain [see comments]. *Nature.* 1996;384(6606):258–260. doi:10.1038/384258a0
11. Wahren LK, Torebjork E, Jorum E. Central suppression of cold-induced C fibre pain by myelinated fibre input. *Pain.* 1989;38(3):313–319. doi:10.1016/0304-3959(89)90218-2
12. Baumgartner U, Magerl W, Klein T, Hopf HC, Treede RD. Neurogenic hyperalgesia versus painful hypoalgesia: two distinct mechanisms of neuropathic pain. *Pain.* 2002;96(1–2):141–151. doi:10.1016/s0304-3959(01)00438-9

13. Yarnitsky D, Ochoa JL. Release of cold-induced burning pain by block of cold-specific afferent input. *Brain*. 1990;113(Pt 4):893–902. doi:10.1093/brain/113.4.893
14. Hallin RG, Torebjork HE. Electrically induced A and C fibre responses in intact human skin nerves. *Exp Brain Res*. 1973;16(3):309–320. doi:10.1007/bf00233333
15. Mackenzie RA, Burke D, Skuse NF, Lethlean AK. Fibre function and perception during cutaneous nerve block. *J Neurol Neurosurg Psychiatry*. 1975;38(9):865–873. doi:10.1136/jnnp.38.9.865
16. Craig AD, Chen K, Bandy D, Reiman EM. Thermosensory activation of insular cortex. *Nat Neurosci*. 2000;3(2):184–190. doi:10.1038/72131
17. Apkarian AV, Bushnell MC, Treede RD, Zubieta JK. Human brain mechanisms of pain perception and regulation in health and disease. *Eur J Pain*. 2005;9(4):463–484. doi:10.1016/j.ejpain.2004.11.001
18. Treede RD, Kenshalo DR, Gracely RH, Jones AK. The cortical representation of pain. *Pain*. 1999;79(2–3):105–111. doi:10.1016/s0304-3959(98)00184-5
19. Price DD. Psychological and neural mechanisms of the affective dimension of pain. *Science*. 2000;288(5472):1769–1772. doi:10.1126/science.288.5472.1769
20. Vogt BA. Pain and emotion interactions in subregions of the cingulate gyrus. *Nat Rev Neurosci*. 2005;6(7):533–544. doi:10.1038/nrn1704
21. Sowards TV, Sowards MA. The medial pain system: neural representations of the motivational aspect of pain. *Brain Res Bull*. 2002;59(3):163–180. doi:10.1016/s0361-9230(02)00864-x
22. Oldfield RC. The assessment and analysis of handedness: the Edinburgh inventory. *Neuropsychologia*. 1971;9(1):97–113. doi:10.1016/0028-3932(71)90067-4
23. Fruhstorfer H, Lindblom U, Schmidt WC. Method for quantitative estimation of thermal thresholds in patients. *J Neurol Neurosurg Psychiatry*. 1976;39(11):1071–1075. doi:10.1136/jnnp.39.11.1071
24. Melzack R. The McGill Pain Questionnaire: major properties and scoring methods. *Pain*. 1975;1(3):277–299. doi:10.1016/0304-3959(75)90044-5
25. Stein C, Mendl G. The German counterpart to McGill Pain Questionnaire. *Pain*. 1988;32(2):251–255. doi:10.1016/0304-3959(88)90074-7
26. Friston KJ, Frith CD, Frackowiak RS, Turner R. Characterizing dynamic brain responses with fMRI: a multivariate approach. *Neuroimage*. 1995;2(2):166–172.
27. Davis KD, Kwan CL, Crawley AP, Mikulis DJ. Functional MRI study of thalamic and cortical activations evoked by cutaneous heat, cold, and tactile stimuli. *J Neurophysiol*. 1998;80(3):1533–1546. doi:10.1152/jn.1998.80.3.1533
28. Maihofner C, Kaltenhauser M, Neundorfer B, Lang E. Temporospatial analysis of cortical activation by phasic innocuous and noxious cold stimuli—a magnetoencephalographic study. *Pain*. 2002;100(3):281–290. doi:10.1016/s0304-3959(02)00276-2
29. Tracey I, Becerra L, Chang I, et al. Noxious hot and cold stimulation produce common patterns of brain activation in humans: a functional magnetic resonance imaging study. *Neurosci Lett*. 2000;288(2):159–162. doi:10.1016/s0304-3940(00)01224-6
30. Craig AD, Zhang ET. Retrograde analyses of spinothalamic projections in the macaque monkey: input to posterolateral thalamus. *J Comp Neurol*. 2006;499(6):953–964. doi:10.1002/cne.21155
31. Kim JH, Greenspan JD, Coghill RC, Ohara S, Lenz FA. Lesions limited to the human thalamic principal somatosensory nucleus (ventral caudal) are associated with loss of cold sensations and central pain. *J Neurosci*. 2007;27(18):4995–5004. doi:10.1523/JNEUROSCI.0716-07.2007
32. Seifert F, Maihofner C. Central mechanisms of experimental and chronic neuropathic pain: findings from functional imaging studies. *Cell Mol Life Sci*. 2009;66(3):375–390. doi:10.1007/s0018-008-8428-0
33. Peyron R. Functional brain imaging: what has it brought to our understanding of neuropathic pain? A special focus on allodynic pain mechanisms. *Pain*. 2016;157(Suppl 1):S67–S71. doi:10.1097/j.pain.0000000000000387
34. Bud Craig AD. Central neural substrates involved in temperature discrimination, thermal pain, thermal comfort, and thermoregulatory behavior. *Handb Clin Neurol*. 2018;156:317–338. doi:10.1016/B978-0-444-63912-7.00019-9
35. Lorenz J, Cross DJ, Minoshima S, Morrow TJ, Paulson PE, Casey KL. A unique representation of heat allodynia in the human brain. *Neuron*. 2002;35(2):383–393. doi:10.1016/s0896-6273(02)00767-5
36. Peyron R, Schneider F, Faillenot I, et al. An fMRI study of cortical representation of mechanical allodynia in patients with neuropathic pain. *Neurology*. 2004;63(10):1838–1846. doi:10.1212/01.wnl.0000144177.61125.85
37. Peyron R, Garcia-Larrea L, Gregoire MC, et al. Allodynia after lateral-medullary (Wallenberg) infarct. A PET study. *Brain*. 1998;121(Pt 2):345–356. doi:10.1093/brain/121.2.345
38. Becerra L, Morris S, Bazes S, et al. Trigeminal neuropathic pain alters responses in CNS circuits to mechanical (brush) and thermal (cold and heat) stimuli. *J Neurosci*. 2006;26(42):10646–10657. doi:10.1523/JNEUROSCI.2305-06.2006
39. Ducreux D, Attal N, Parker F, Bouhassira D. Mechanisms of central neuropathic pain: a combined psychophysical and fMRI study in syringomyelia. *Brain*. 2006;129(Pt 4):963–976. doi:10.1093/brain/awl016
40. Lebel A, Becerra L, Wallin D, et al. fMRI reveals distinct CNS processing during symptomatic and recovered complex regional pain syndrome in children. *Brain*. 2008;131(Pt 7):1854–1879. doi:10.1093/brain/awn123
41. Bouhassira D, Kern D, Rouaud J, Pelle-Lancien E, Morain F. Investigation of the paradoxical painful sensation ('illusion of pain') produced by a thermal grill. *Pain*. 2005;114(1–2):160–167. doi:10.1016/j.pain.2004.12.014
42. Seifert F, Maihofner C. Representation of cold allodynia in the human brain—a functional MRI study. *Neuroimage*. 2007;35(3):1168–1180. doi:10.1016/j.neuroimage.2007.01.021
43. Leijon G, Boivie J, Johansson I. Central post-stroke pain—neurological symptoms and pain characteristics. *Pain*. 1989;36(1):13–25. doi:10.1016/0304-3959(89)90107-3
44. Klit H, Finnerup NB, Jensen TS. Central post-stroke pain: clinical characteristics, pathophysiology, and management. *Lancet Neurol*. 2009;8(9):857–868. doi:10.1016/S1474-4422(09)70176-0
45. Namer B, Kleggetveit IP, Handwerker H, Schmelz M, Jorum E. Role of TRPM8 and TRPA1 for cold allodynia in patients with cold injury. *Pain*. 2008;139(1):63–72. doi:10.1016/j.pain.2008.03.007
46. Wasner G, Naleschinski D, Binder A, Schattschneider J, McLachlan EM, Baron R. The effect of menthol on cold allodynia in patients with neuropathic pain. *Pain Med*. 2008;9(3):354–358. doi:10.1111/j.1526-4637.2007.00290.x
47. Sundstrup E, Jakobsen MD, Brandt M, et al. Acute effect of topical menthol on chronic pain in slaughterhouse workers with carpal tunnel syndrome: triple-blind, randomized placebo-controlled trial. *Rehabil Res Pract*. 2014;2014:310913. doi:10.1155/2014/310913
48. Gonzalez A, Ugarte G, Restrepo C, et al. Role of the excitability brake potassium current IKD in cold allodynia induced by chronic peripheral nerve injury. *J Neurosci*. 2017;37(12):3109–3126. doi:10.1523/JNEUROSCI.3553-16.2017
49. Viana F. Nociceptors: thermal allodynia and thermal pain. *Handb Clin Neurol*. 2018;156:103–119. doi:10.1016/B978-0-444-63912-7.00006-0
50. Belmonte C, Brock JA, Viana F. Converting cold into pain. *Exp Brain Res*. 2009;196(1):13–30. doi:10.1007/s00221-009-1797-2
51. Sittl R, Lampert A, Huth T, et al. Anticancer drug oxaliplatin induces acute cooling-aggravated neuropathy via sodium channel subtype Na (V)1.6-resurgent and persistent current. *Proc Natl Acad Sci U S A*. 2012;109(17):6704–6709. doi:10.1073/pnas.1118058109
52. Hansson P, Baron R, Stubhaug A. Acute neuropathic pain: equivalent or different to chronic neuropathic pain? A call for gathering of scientifically based information on acute neuropathic pain. *Pain*. 2019;1. doi:10.1097/j.pain.0000000000001650

Journal of Pain Research

Dovepress

Publish your work in this journal

The Journal of Pain Research is an international, peer reviewed, open access, online journal that welcomes laboratory and clinical findings in the fields of pain research and the prevention and management of pain. Original research, reviews, symposium reports, hypothesis formation and commentaries are all considered for publication. The manuscript

management system is completely online and includes a very quick and fair peer-review system, which is all easy to use. Visit <http://www.dovepress.com/testimonials.php> to read real quotes from published authors.

Submit your manuscript here: <https://www.dovepress.com/journal-of-pain-research-journal>